Perpendicular-to-grain dowel-bearing strength behavior of side pressure laminated bamboo lumber

Tingting Ling [1,2], Haitao Li[1,2*], Gensheng Cheng[1,2], Zhenhua Xiong[3], Rodolfo Lorenzo[4]

[1] College of Civil Engineering, Nanjing Forestry University, Nanjing 210037, China;

[2] Joint International Research Laboratory for Bio-composite Building Materials and Structures, Nanjing Forestry University, Nanjing 210037, China

[3] Ganzhou Sentai bamboo company LTD, Ganzhou 341001, China.

[4] University College London, London WC1E 6BT, UK.

*Corresponding author: Haitao Li, Professor, E-mail: lhaitao1982@126.com

Abstract: Research on dowel-bearing strength is an indispensable part of bolt connections. The size effect (length, width, and thickness), bolt diameter, and the arrangement of bamboo units are examined in this research, to study their influence on the dowel-bearing behavior of side pressure laminated bamboo lumber (LBL). The test results show that when the specimen length and width are 5 times larger than the bolt diameter, and the thickness is 3 times larger than the bolt diameter, the dowel-bearing strength of the specimen tends to be stable. The stiffness of the standard size specimen (80 mm × 80 mm × 40 mm) reaches the minimum at 16 mm of bolt diameter, and the dowel-bearing strength remains stable after 16 mm of the bolt diameter. The increase in the specimen thickness can enhance the ability of the specimen to oppose deformation. Comparing the two different arrangements of bamboo units, it is found that the strength and stiffness of the specimen with a horizontal arrangement (ZRT) are lower than those with a vertical arrangement (ZTR). Finally, a new formula to predict the perpendicular-to-grain dowel-bearing strength of side pressure LBL is reconstructed based on existing specifications.

Keywords: A. Laminated bamboo lumber, B. Dowel-bearing strength, C. Bolt connections, D. Size effect

1 Introduction

Bamboo has superior environmental properties, and it can mature within 3-4 years [1], while wood takes more than 20 years to mature [2]. Bamboo holds the characteristics of a large amount of carbon storage, and low energy consumption during processing, and it can be degraded after waste [3]. However, the original bamboo has the disadvantages of small diameter, thin hollow wall, large taper, uneven structure, and the variability of geometric size and mechanical properties, which limits its application in civil engineering [4, 5].

Engineered bamboo [6], such as laminated bamboo lumber (LBL) [7], glubam[8], bamboo scrimber

[9], and laminated flattened-bamboo lumber (LFBL) [10], can overcome these natural defects of the original bamboo, and they have great advantages in carbon emissions and production energy consumption. The treatment of original bamboos such as flattening technology [11], bonding methods [12], and heat treatment [13] was improved, which promoted the application process of engineered bamboo. Fig. 1 shows the comparison of environmental performance between some engineered bamboo and other engineering materials. The global forest cover is decreasing and the demand for wood is increasing, so exploring bamboo instead of wood to apply to structures is a good way to alleviate this problem [14].
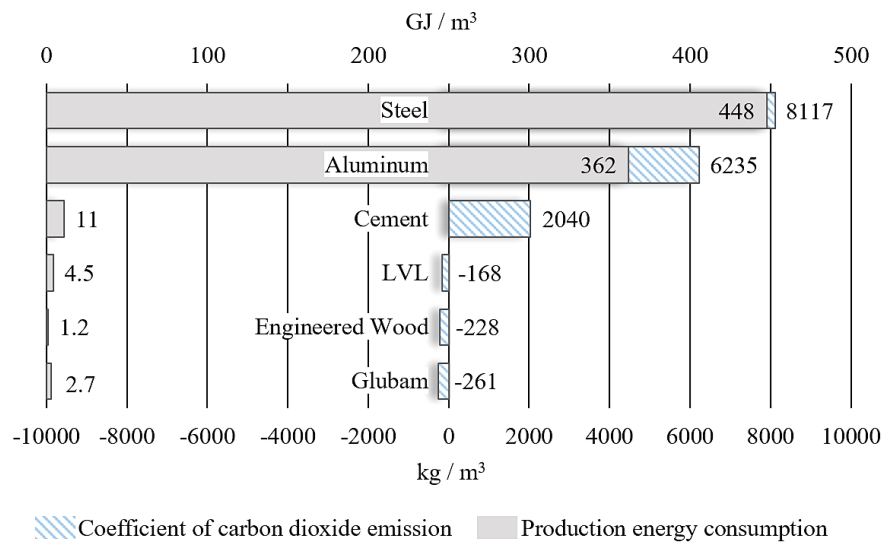
GJ / m^3

Fig. 1 Comparison of environmental performance between different building materials [15]

Fig. 2 shows the process of side pressure LBL: the bamboo is broken into fixed width and thickness of strips, the green surface of bamboo and yellow internal of the bamboo are removed, and dried to a moisture content of 8 % ~ 12 %, finally, the bamboo unites are pressed longitudinally and transversely and glued with adhesive [16]. The basic material properties of LBL were researched and analyzed. Li et al. [17, 18] researched the flexural and compressive performance of laminated bamboo, and based on these studies, they believed that laminated bamboo is a suitable construction material for engineering structures. Sulastiningsih [19] found that laminated bamboo board (LBB) had the potential as a wood substitute. Compared with wood, Verma's research [20] indicated that the strength of bamboo laminae was better than softwoods and comparable with hardwood. Li and Chen's research [21] manifested that the mechanical properties of LBL columns can be enhanced by wrapping fiber-reinforced polymer (FRP) on the surface. All these studies show that exploring the potential abilities of LBL is a hot topic of current research, and the bamboo components applied to bridges and residences also make it possible to explore more possibilities of LBL [22, 23].

Pin joints including nail joints and bolted joints are broadly applied in wood structures. About 80 % of structural failures were caused by the connection's damage. The failure of joints is mainly manifested in the bending failure of bolts and the compression failure of the dowel [24]. In 1991, the United States introduced "Yield Theory" into the design code of wood structure, and proposed the theoretical calculation formula which is closely related to the dowel-bearing strength. Numerous factors such as bolt diameter, wood density, loading direction, wood moisture content, temperature change, and the connector type influence the dowel-bearing strength. Smith et al. [25] studied the effects of 7 different species of wood on the dowel-bearing performance, and Rammer et al. [26] developed a linear relationship between dowel-bearing strength and moisture content of Southern Pine pieces. Hwang et al. [27] tested the dowel-bearing strength with divers bolts of 4 species of laminated materials, and the results showed that the dowel-bearing strength is independent of bolt diameter. Sosa' research [28] displayed that different measurements would lead to different results in dowel-bearing strength. Li [29] found that there were relationships between the dowel-bearing behaviors and the fiber angle of LBL, the stiffness and strength of the dowel specimen were at the lowest value when the fiber angle was 60 °.
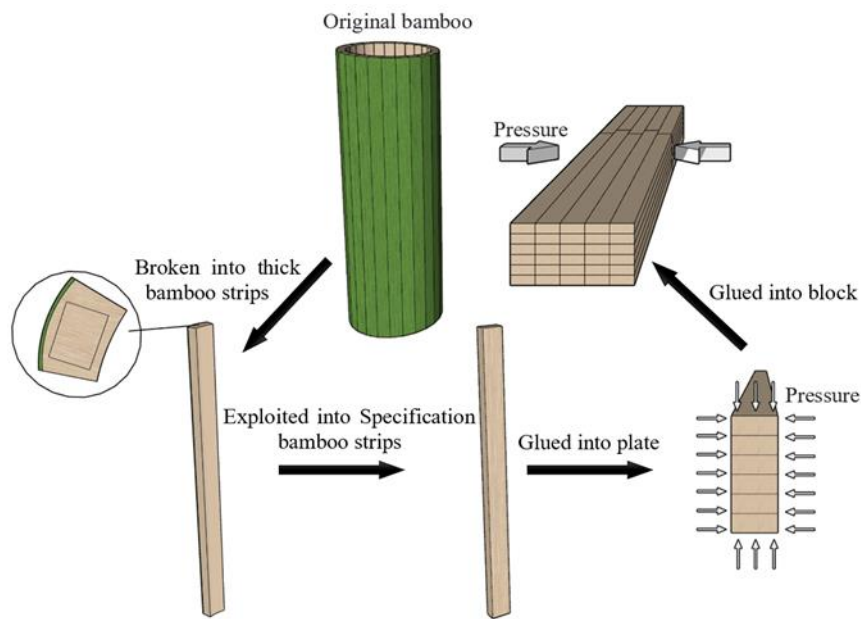

Fig. 2 The processing of side pressure LBL

There are often both bending moment and shear force at the nodes of bamboo and wood structures, which is therefore difficult to determine the extrusion direction of bolts and holes. The orientation of the bamboo fiber arrangement determines that the bearing capacity of bamboo is quite different in the direction of parallel and perpendicular grains [30, 31]. Sawata et al. [32] found that parallel and perpendicular to the

grain have different embedding strengths, and the embedding strength parallel-to-grain was 0.9 times as large as the compressive strength, while the embedding strength perpendicular-to-grain was 4 times as large as the compressive strength perpendicular-to-grain.

The bolted and holes are easy to squeeze each other, as a result, brittle failure occurs at the dowel because of the local tensile stress in the perpendicular direction, and the macroscopic performance is the splitting failure of the bolt holes along the perpendicular direction, and this kind of damage always occurs before other forms of destruction [33]. Bolt joints are usually assumed to be hinged, due to this assumption, researchers focus less on perpendicular-to-grain dowel-bearing strength. Further studies about the behavior of perpendicular-to-grain dowel-bearing strength should be processed to improve this situation.

2 Materials and methods

2.1 Materials

The materials employed in the research include side pressure LBL and bolt rods. Side pressure LBL was processed by Ganzhou Sentai bamboo company in Jiangxi Province. The original bamboo species is Moso bamboo (Phyllostachys pubescens), and the size of bamboo units is 2005 mm × 21 mm × 7 mm. The bamboo units were pressed into side pressure LBL with resorcinol as the adhesive at a temperature of 157 ℃ and under main pressure of 9 MPa and lateral pressure of 6.5 MPa. 10 specimens were randomly selected to measure the size and mass for calculating the density, and the density of the material is about 0.672 g / cm^3. The 10 specimens were then dried in an oven and weighed again to calculate the moisture content, and the moisture content is about 9.10 %. The bolt rod was composed of Q235 with a smooth surface. Five different diameters of bolt rods are selected, which are 12 mm, 14 mm, 16 mm, 18 mm, and 20 mm.

2.2 Specimen design and fabrication

2.2.1 Specimen of perpendicular-to-grain dowel-bearing strength

Side pressure LBL is a new material used in structures since the test standards, and procedures have not been formulated. Considering that side pressure LBL and wood have similar mechanical properties, the test method suitable for wood is used in this research. The current test method for determining the dowel-bearing strength of wood is mainly based on ASTM-D5764-97a [34] and BS EN 383-2007 [35]. The former provides details of the process and requirements of the half-hole test and full-hole test of wood dowel-bearing strength, while the latter only involves full-hole tests.

Fig. 3 illustrates the two different test methods mentioned above. The load is applied to the bolt by the

moving platform of the test machine in the half-hole test so that the bolt is subjected to uniform load in the length direction, then the compression is transferred to the inside of the dowel. The specimen should be located in the center of the platform so that the load will be vertically and symmetrically relative to the specimen. The loading point of the full-hole test is at the end of the bolt, and the bolt is more likely to bend. Compared with the full-hole test, the bolt in the half-hole test is prone to maintain rigidity so that the test results can more accurately reflect the bearing strength of the whole groove. So half-hole test is comprehensively regarded to be used in this test.
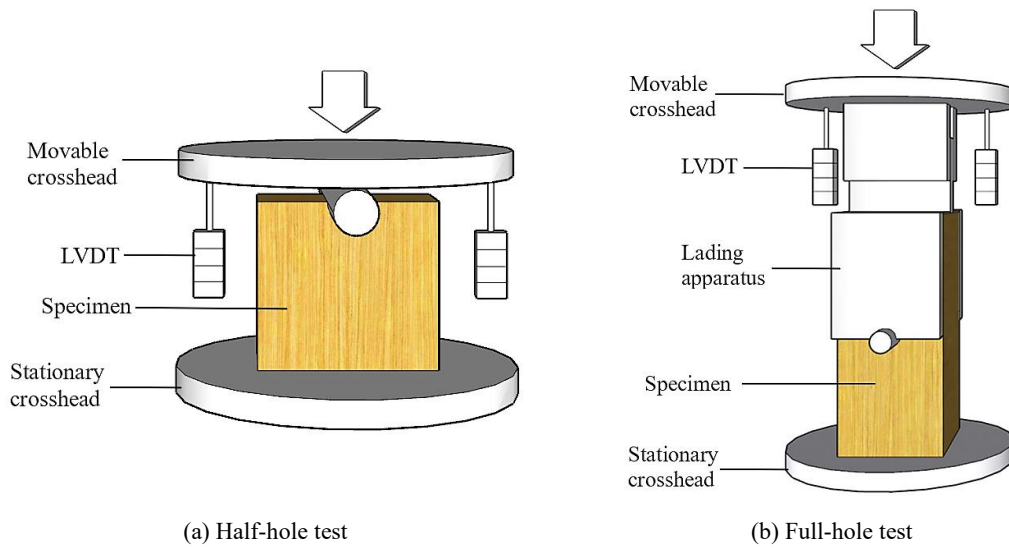

| (a) Half-hole test | (b) Full-hole test |

Fig. 3 Schematic diagram of the test method

Table 1 Influence factors and levels

Factors	Arrangement	Level	Value (mm)	Groups	Arrangement	Level	Value (mm)	Groups
Length		1	60	ZRTL60		1	60	ZTRL60
		2	70	ZRTL70		2	70	ZTRL70
		3	80	ZRTS		3	80	ZTRS
		4	90	ZRTL90		4	90	ZTRL90
		5	100	ZRTL100		5	100	ZTRL100
Width		1	60	ZRTW60		1	60	ZTRW60
		2	70	ZRTW70		2	70	ZTRW70
		3	80	ZRTS		3	80	ZTRS
		4	90	ZRTW90		4	90	ZTRW90
	Horizontal (ZRT)	5	100	ZRTW100	Vertical (ZTR)	5	100	ZTRW100
Thickness		1	30	ZRTT30		1	30	ZTRT30
		2	35	ZRTT35		2	35	ZTRT35
		3	40	ZRTS		3	40	ZTRS
		4	45	ZRTT45		4	45	ZTRT45
		5	50	ZRTT50		5	50	ZTRT50
Diameter		1	12	ZRTD12		1	12	ZTRD12
		2	14	ZRTD14		2	14	ZTRD14
		3	16	ZRTS		3	16	ZTRS
		4	18	ZRTD18		4	18	ZTRD18
		5	20	ZRTD20		5	20	ZTRD20

The current specimen was manufactured according to the requirements of ASTM-D5764-97a [34] for the half-hole test. After cutting, drilling, and grinding, the specimen of side pressure LBL perpendicular-to-

grain dowel-bearing strength was finished (Fig. 4). The diameter of the hole is 1 mm larger than the diameter of the bolt rod, and the allowable error of the length, width, and thickness of the sample are ± 0.5 mm.

According to the different arrangement of bamboo units, the specimens of perpendicular-to-grain dowel test were divided into 2 types, namely ZRT and ZTR (Fig. 5). In addition, other influence factors are set to five levels, among which the specimen with length × width × thickness as 80 mm × 80 mm × 40 mm and the bolt diameter as 16 mm is the standard specimen, the changes of different factors are all based on this specimen. There are two groups of standard specimens, ZRTS and ZTRS. If a group of specimens is named ZRTT40, which represents that the variable of this group of specimens is thickness, and the thickness of this group is 40 mm, the loading direction is perpendicular to the bamboo unit, and the other parameters are the same as the standard specimens. The design parameters and groups of specimens are given in Table 1, and the test consisted of 34 sets of six specimens each, for a total of 204 specimens.
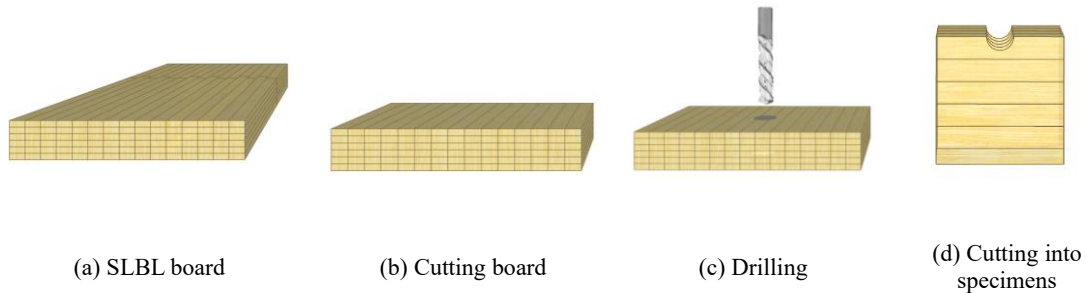

| (a) SLBL board | (b) Cutting board | (c) Drilling | (d) Cutting into specimens |

Fig. 4 Manufacturing process of the dowel-bearing strength specimen

| (a) ZRT | (b) ZTR |

Note: L is the length of the specimen, W is the width of the specimen, T is the thickness of the specimen, and D is the diameter of the bolt rod.

Fig. 5 Characteristics of the specimens

2.2.2 Specimen of perpendicular-to-grain compressive strength

To study the relationship between the compressive strength and dowel-bearing strength of perpendicular-to-grain side pressure LBL, 40 compressive specimens were manufactured using the same materials as the dowel-bearing strength specimen, of which 20 specimens were arranged in ZRT and ZTR respectively. The specimen was designed and loaded according to ASTM D143-97 [34], and the length of the specimen is 100 mm and the cross-section is a square of 50 mm. The diagram of the specimen and the

loading method are shown in Fig. 6.

The loading device was a 200-ton microcomputer controlled electro-hydraulic servo universal testing machine, and the test was controlled by displacement with a speed of 1.5 mm / min. When the load dropped to 80 % of the ultimate load, the test should be stopped. The steps of the test: (1) strain gauges were pasted, and both ends of the specimens were polished with sandpaper to reduce the hoop effect caused by end friction; (2) after the specimen was placed on the platform, the geometric alignment was first performed to align the action line of the load with the geometric center of the component to ensure axial compression; (3) the specimen was preloaded to detect whether the instrument was working properly, and reduce the system error; (4) formally loaded, observe and record the test phenomenon, photographed until the end of the test. The experimental results showed that the perpendicular-to-grain compressive strength of ZRT is 20.52 MPa and ZTR is 24.96 MPa, and the coefficients of variation (COV) are 6.2% and 2.1%, respectively.
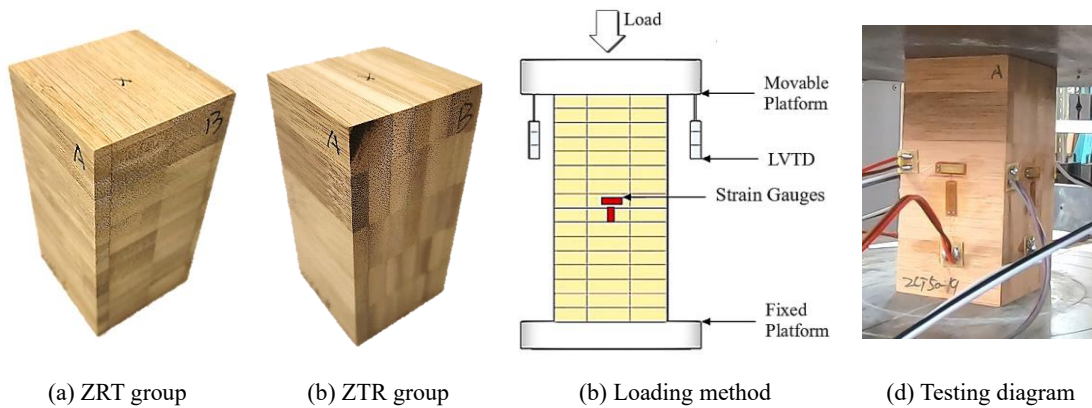

| (a) ZRT group | (b) ZTR group | (b) Loading method | (d) Testing diagram |

Fig. 6 Specimen and process of the compressive strength test

2.3 Test method

The half-hole test was completed in the civil engineering structure laboratory of Nanjing Forestry University. The loading device was a 10-ton microcomputer controlled electro-hydraulic servo universal testing machine (Fig. 7 (a)). In the test, the specimen was first placed on the bearing platform, and the center of the specimen is aligned with the center of the platform. Then the bolt was placed lightly into the dowel, and the bolt should be symmetrically placed on both sides of the dowel, that is, the extension distance of the bolts on both ends should be equal (Fig. 7 (b)). After the specimen was placed appropriately, the test device was operated to make the surface of the moving platform contact with the highest point of the bolt, and the contact forces should be less than 1 kN. The loading speed was 1.5 mm / min, and the test process of each sample lasted about 5 ~ 8 minutes. When the specimen showed obvious damage or the bearing capacity decreased to 80 % of the peak value or the bolt was completely embedded in the specimen (Fig. 7 (c)), the test would be stopped. It was noted that there was no noticeable failure phenomenon when all the

specimens reached the ultimate bearing capacity. At this time, the bolt was completely embedded in the specimen, and the test stopped.
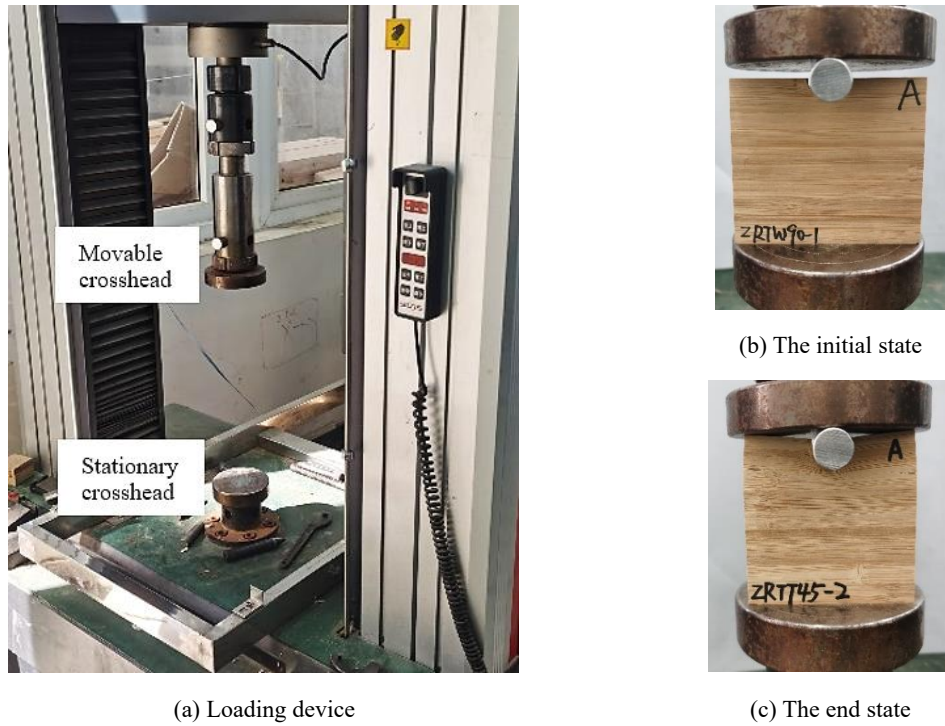

(a) Loading device

(b) The initial state

(c) The end state
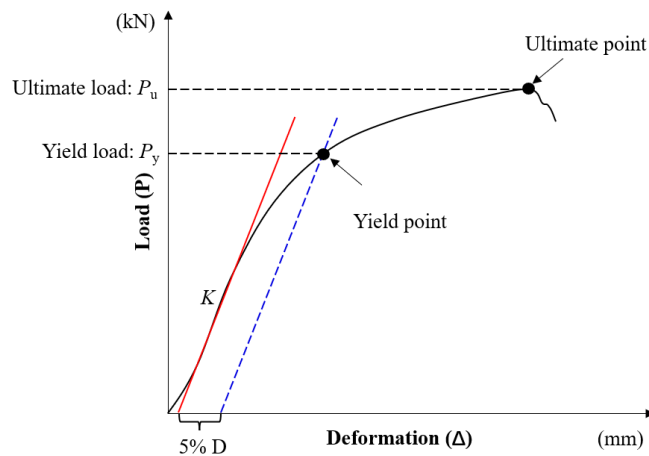
Fig. 7 Test device and states

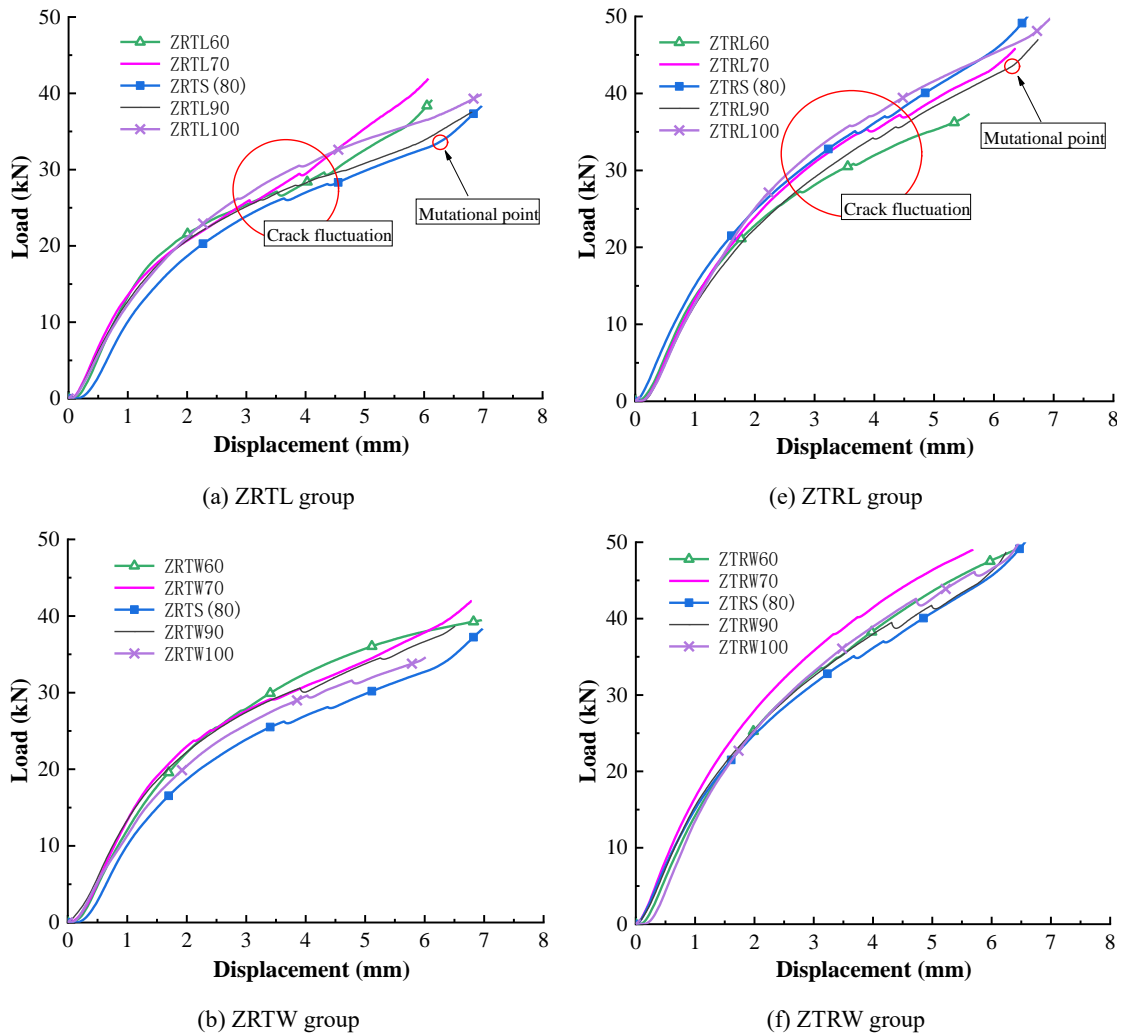Fig. 8 5％D offset method for evaluating the yield load of the specimen

According to ASTM-D5764-97a [34], the yield strength is deemed to be the dowel-bearing strength. The stiffness can be determined from the linear slope of the load-displacement curve over 10 % P_{max} and 40 % P_{max} (P_{max} is the maximum load value in the test process). The straight line is translated to the right, and the translation value is 5 % of the bolt diameter. The ordinate of the intersection point between the translated straight line and the test curve is the value of yield load. Fig. 8 shows the action process of the 5% D offset method, and MATLAB (a data processing software) was used to obtain the initial stiffness (K) and the yield load (P_y) of each specimen.

8

3 Results and Discussion

3.1 Failure mode and analysis

3.1.1 Load-displacement curves and failure process

Fig. 9 shows that the load-displacement curve is nonlinear at first because of the initial gap between the bolt and the specimen. With the increase in load, the initial gap is eliminated, and the curve enters the linear stage. Then the plastic deformation occurs, and the curve enters the nonlinear stage. Due to the stress concentration at both ends of the semi-circular hole, the bamboo fiber perpendicular to the load direction The specimen maintained good ductility, and the bolt had no obvious bending deformation in the test. gradually bends, and the pressure-bearing area sinks and bulges outward. The load decreases slightly when the displacement reaches about 3.5 mm since a lateral crack first appears.

(a) ZRTL group

(e) ZTRL group

(b) ZRTW group

(f) ZTRW group

(c) ZRTT group

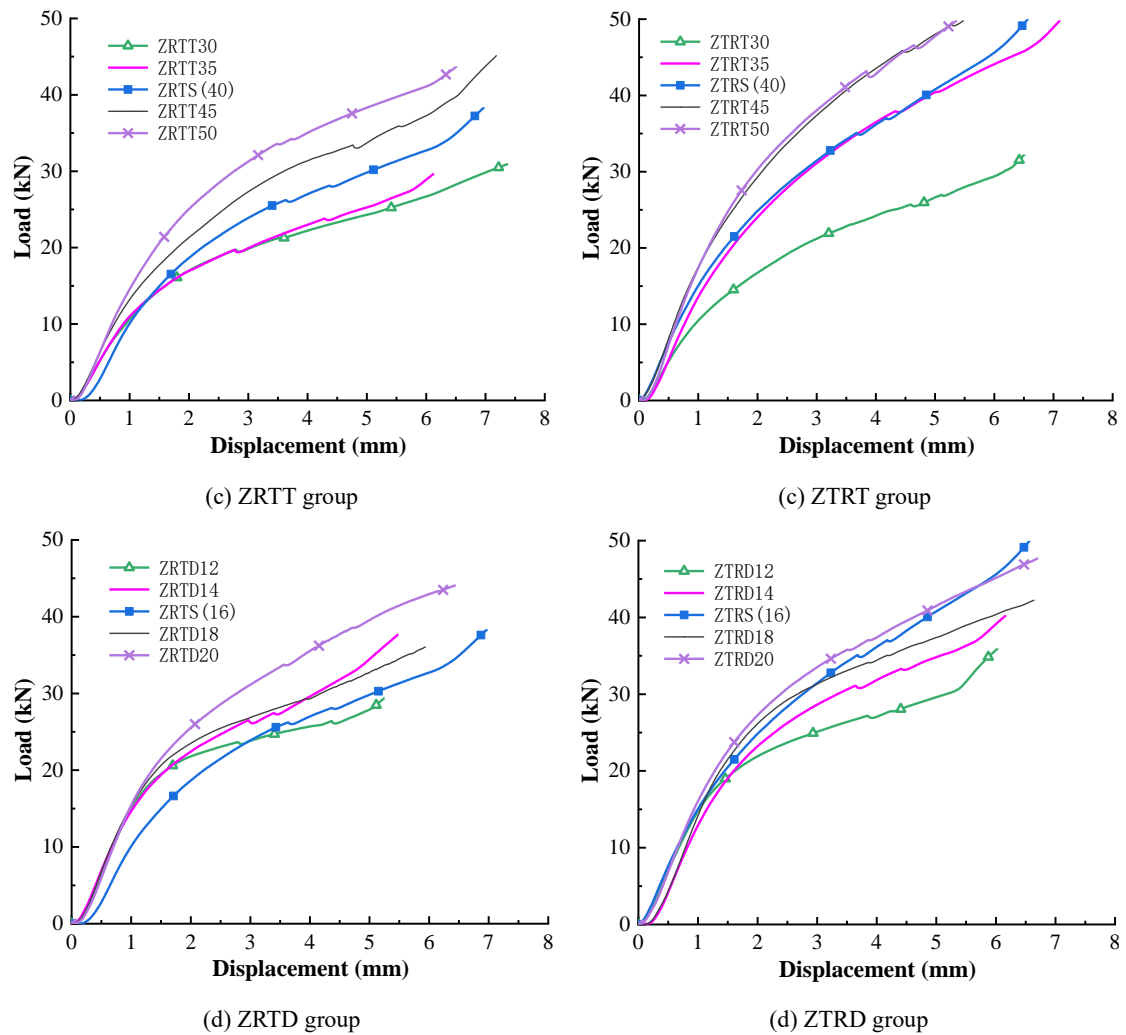(c) ZTRT group

(d) ZRTD group

(d) ZTRD group

Fig. 9 Load-displacement typical curve

Subsequently, the bearing capacity continues to rise until the displacement reaches about 4.5 mm, and there appears a second load drop accompanied by another lateral crack. The cracks on both sides of the specimen spread to the center of the specimen, and the material above the cracks warped up. There was internal compression at the bottom of the dowel and tensile at both ends of the specimens in the width direction, and local compression failure of the bamboo lumber under the bolt occurred, resulting in the misalignment of the vascular bundle (Fig. 10). Owing to the strong deformation ability of the specimen, when the bolt is completely embedded in the groove, the specimen has not been destroyed, so the curve has no significant decline stage. Only when the lateral crack appears, there is a slight loading decline. Finally, when the loading platform is in contact with the top of the specimen, the displacement-load curve changes abruptly, and the specimen changes from local compression to overall compression, which means that the test stops.

Although the load-displacement curves and failure processes (Fig. 11, Fig. 12) of the two kinds of specimens are similar, when the lateral cracks appear, the ZRT groups are faster than the ZTR groups, and

the lateral crack propagates faster, which manifests that the ductility of ZTR groups is better. Whenever the bearing capacity decreases, the load of ZRT groups is generally lower than that of ZTR groups, so the bearing capacity of ZTR groups is better and the stiffness is greater than that of ZRT groups. This phenomenon is not only shown in the elastic stage, after the yield point, until the failure of the specimen, and ZTR groups continue the phenomenon of higher stiffness.
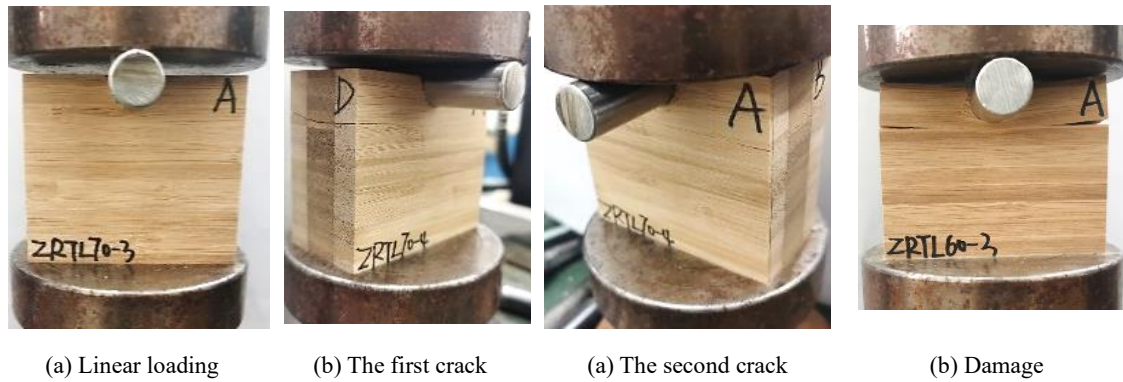

| (a) ZRT | (b) ZTR |

Fig.10 Misalignment of the vascular bundle

| (a) Linear loading | (b) The first crack | (a) The second crack | (b) Damage |

Fig. 11 The failure process of the ZRT specimen

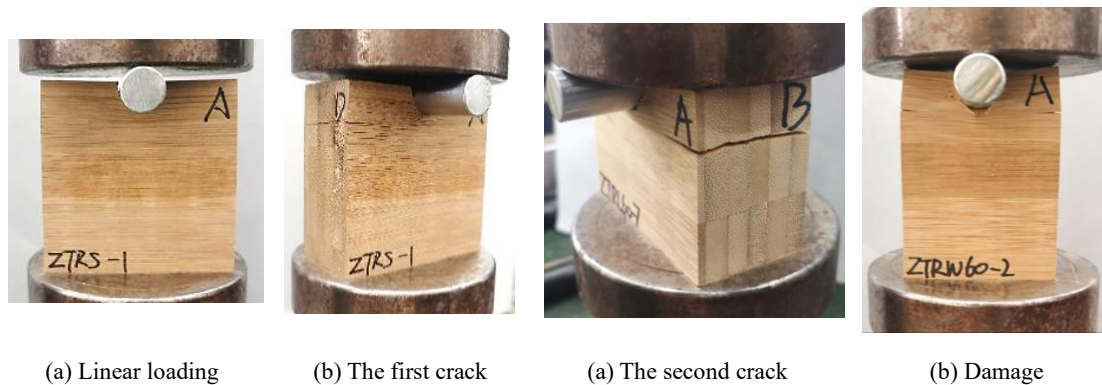| (a) Linear loading | (b) The first crack | (a) The second crack | (b) Damage |

Fig. 12 The failure process of the ZTR specimen

3.1.2 Failure mode

The failure characteristics of all specimens were consistent in the form of A and C surfaces, and the difference was only shown in the lateral cracks of B and D surfaces. Therefore, the form of side cracks is classified into six failure modes.

Mode 1: The angle between the lateral crack and the horizontal plane of the ZRT specimen was

between 0 ° and 15 ° (Fig. 13 (a)).

Mode 2: The angle between the lateral crack and the horizontal plane of the ZRT specimen was between 15 ° and 30 ° (Fig. 13 (b)).

Mode 3: The lateral crack of the ZRT specimen expanded from one to two (Fig. 13 (c)).

Mode 4: The lateral crack of the ZTR specimen was penetrative (Fig. 13 (d)).

Mode 5: Split layer crack occurred on the lateral surface of the ZTR specimen (Fig. 13 (e)).

Mode 6: The lateral crack of the ZTR specimen expanded from one to two (Fig. 13 (f)).

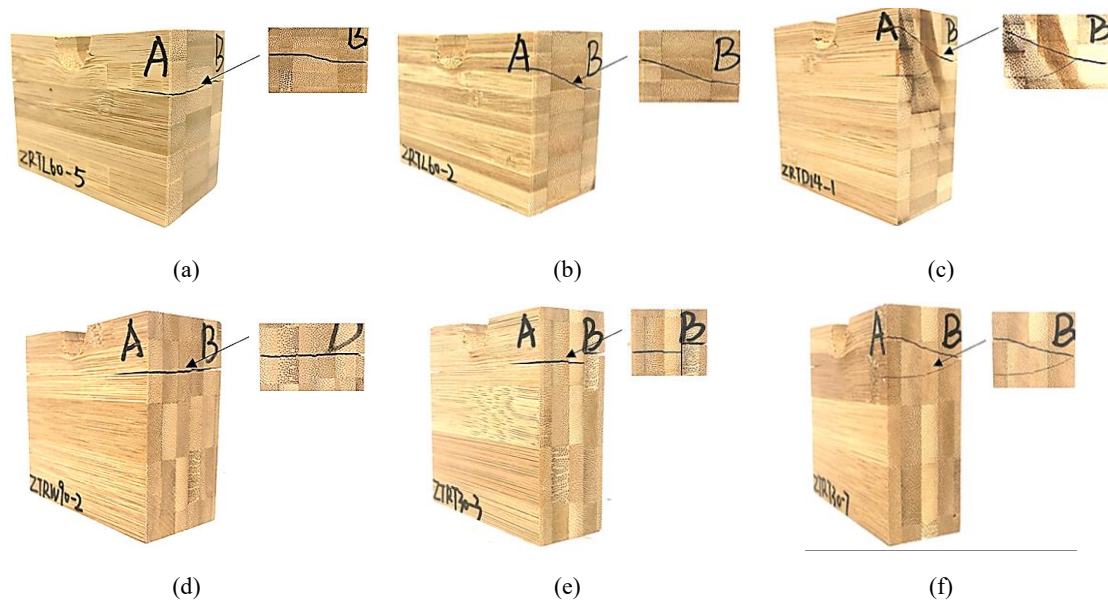|		
(a)	(b)	(c)
(d)	(e)	(f)

Fig.13 Classification of failure modes

According to the analysis and statistics of the failure modes of the lateral cracks of all the specimens, Fig. 14 is obtained. It can be found that the main failure modes of lateral cracks are penetrative flat cracks, reaching 86.03 % of the total number. The probability of mode 2 is the smallest. Mode 3 and mode 6 accounted for the second place, and the proportions are 3.92 % and 4.41 % respectively. Due to the failure of bamboo to reach a shear strength, the lateral cracks expand from one to two. For ZRT specimens, the specimens with a larger length-thickness ratio and width-thickness ratio seem to be more prone to cracks with larger inclination angles.

3.1.3 Cause and analysis of failure

The ductility of the ZRT specimen is better than the ZTR specimen. The reason for this difference is primarily that the adhesive layer distribution of the two kinds of specimens is different. In the length direction, the adhesive layer distribution of the ZRT sample is relatively close, and when the bottom of the dowel was compressed, the stress near the horizontal plane in the vertical direction of the bottom of the

dowel is large, the location of the crack is near the horizontal plane. However, the adhesive layer is the weak surface of LBL to resist the load, and the adhesive layer separation was easy to occur at the stress concentration. Compared with the ZTR specimen, the distribution of the adhesive layer in the length direction is relatively sparse, and generally, there is no adhesive layer near the horizontal plane in the vertical direction at the bottom of the dowel, so the lateral crack of the ZTR specimen occurred in the interior of the bamboo strip unit, rather than in the adhesive layer, and the crack is generally flat, which is the reason why the crack extension of ZTR specimen was milder than that of ZRT specimen.
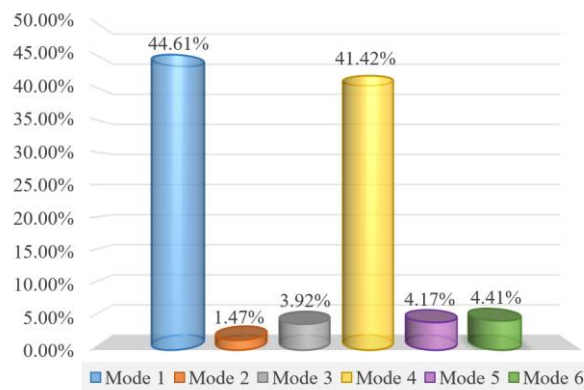

Fig.14 Statistical diagram of failure modes

The control factor of the lateral crack in mode 1 was the horizontal adhesive layer of the intermediate bamboo unit in the thickness direction. Since the horizontal middle adhesive layer has a large coating area, the force required for its failure is large enough to reach the tensile strength of the bamboo. Therefore, the crack appeared from the edge of the bamboo fiber to the adhesive layer of the intermediate bamboo fiber, and the angle of the crack is small. The control factor of mode 2 was the adhesive layer of the edge bamboo unit in the thickness direction. After the edge bamboo unit adhesive layer cracks, due to the small force, it cannot reach the strength of the middle adhesive layer, so a diagonal oblique crack is formed in the middle bamboo unit, which causes the shear failure of the middle bamboo unit. The reason for the first development of mode 3 lateral crack was similar to that of mode 2, which was the tensile cracking of the edge adhesive layer, but the cracking position is different. The crack position relative to the position of the middle bamboo unit determines the crack propagation form. When the edge crack extended to the middle layer, it was located in the middle of the length of the bamboo unit, and the middle bamboo unit reaches the shear strength on the oblique section, so the crack extends from one to two. If the position of the edge crack propagation is the end of the length of the middle bamboo unit, only one shear crack will be formed along the middle bamboo unit, which formed mode 2.

Mode 4 was a tensile failure of side pressure LBL on both sides of the non-compression zone, and the

connection between bamboo units and adhesive layers was relatively uniform, which formed a penetrating lateral crack. The reason for the formation of cracks in mode 5 was the same as that in mode 4, but due to manual glue coating, it may lead to the uneven plane adhesive layer with a large area, so that the cracks cannot penetrate and form staggered cracks. The form of lateral inclined cracks such as mode 6 was caused by insufficient shear strength of the bamboo unit, then the cracks extended from one tensile crack to two shear cracks.

3.2 Stiffness and yield strength

Table 2 Test results of perpendicular-to-grain dowel-bearing properties of side pressure LBL

Factors (ZRT)	Level (mm)	Stiffness (kN / mm)	Yield Strength (MPa)	Factors (ZTR)	Level (mm)	Stiffness (kN / mm)	Yield Strength (MPa)
L	60	18.45 (8.16)	37.13 (8.63)	L	60	17.99 (2.79)	39.52 (11.10)
	70	17.52 (7.88)	36.15 (5.59)		70	17.76 (3.40)	45.09 (4.46)
	80	15.64 (8.24)	35.41 (7.05)		80	17.45 (4.31)	44.03 (4.60)
	90	16.64 (9.77)	39.18 (4.39)		90	17.73 (2.72)	42.56 (3.26)
	100	16.12 (3.84)	37.43 (2.75)		100	17.44 (2.19)	44.11 (5.92)
W	60	15.40 (4.99)	35.14 (8.35)	W	60	18.10 (3.70)	47.34 (9.17)
	70	15.69 (13.34)	34.98 (13.95)		70	19.43 (7.87)	48.45 (8.51)
	80	15.64 (8.24)	35.41 (7.05)		80	17.45 (4.31)	44.03 (4.60)
	90	15.56 (7.37)	37.09 (7.56)		90	19.08 (5.42)	46.79 (7.20)
	100	15.39 (9.50)	35.92 (12.00)		100	19.02 (3.22)	53.29 (8.19)
T	30	13.20 (9.23)	36.80 (4.74)	T	30	14.35 (4.19)	39.45 (5.86)
	35	14.58 (1.62)	35.37 (10.13)		35	18.31 (4.26)	51.33 (3.79)
	40	15.64 (8.24)	35.41 (7.05)		40	17.45 (4.31)	44.03 (4.60)
	45	17.07 (4.83)	31.78 (11.79)		45	22.10 (3.06)	49.97 (4.49)
	50	18.87 (3.78)	36.43 (3.15)		50	23.60 (1.87)	44.41 (2.82)
D	12	19.90 (2.19)	44.19 (6.71)	D	12	19.31 (4.81)	48.66 (7.96)
	14	18.23 (3.82)	38.18 (6.34)		14	18.24 (2.61)	46.17 (3.17)
	16	15.64 (8.24)	35.41 (7.05)		16	17.45 (4.31)	44.03 (4.60)
	18	20.67 (9.76)	36.09 (12.48)		18	19.87 (4.09)	44.68 (4.47)
	20	19.60 (5.15)	38.00 (4.54)		20	21.00 (4.22)	44.59 (12.01)

Note: The number in parentheses is the corresponding coefficient of variation (%).

From the test results, it can be observed that the ductility of side pressure LBL perpendicular-to-grain dowel specimens under compression is good, and the bolt was almost completely embedded into the specimen when the failure occurs. Therefore, when calculating the perpendicular-to-grain dowel yield strength, the bearing surface area is the product of specimen thickness and bolt diameter. The yield strength can be obtained by Eq. (1). The test results of each group were detailed in Table 2.

$$f_y = \frac{P_y}{dt} \tag{1}$$

Where f_y is yield strength, P_y is yield load, d is bolt diameter (the average width of compression bearing surface), t is the thickness of specimens

The stiffness of the perpendicular-to-grain specimens varies from 13.20 to 23.60 kN / mm, and the coefficient of variation is within 13.34 %. The yield strength fluctuates in the range of 31.78 ~ 53.29 MPa,

and the coefficient of variation is less than 13.95 %. It is generally stipulated that for the mechanical parameters of biomass materials, the coefficient of variation is less than 20 %, which can be regarded as effective. It can be found that the coefficient variation of the stiffness and yield strength of ZRT groups is generally higher than that of ZTR groups. This is because, in the unit length, the distribution of the adhesive layer of ZRT groups is denser than that of ZTR groups, when the LBL is being manufactured, there are many factors such as the uneven thickness of the adhesive layer, different aging time after the glue coating, and so on. The uncontrollable factors of ZRT groups are more than those of ZTR groups, so the test values between ZRT specimens fluctuate greatly.

3.3 Size effect

Fig. 15 (a) indicates that in the range of 60 ~ 100 mm, there is no obvious relationship between the length and the stiffness and yield strength of the specimens, which was consistent with Rammer's [26] test results under multiple moisture content conditions.

(a) Effect of length

(b) Effect of width

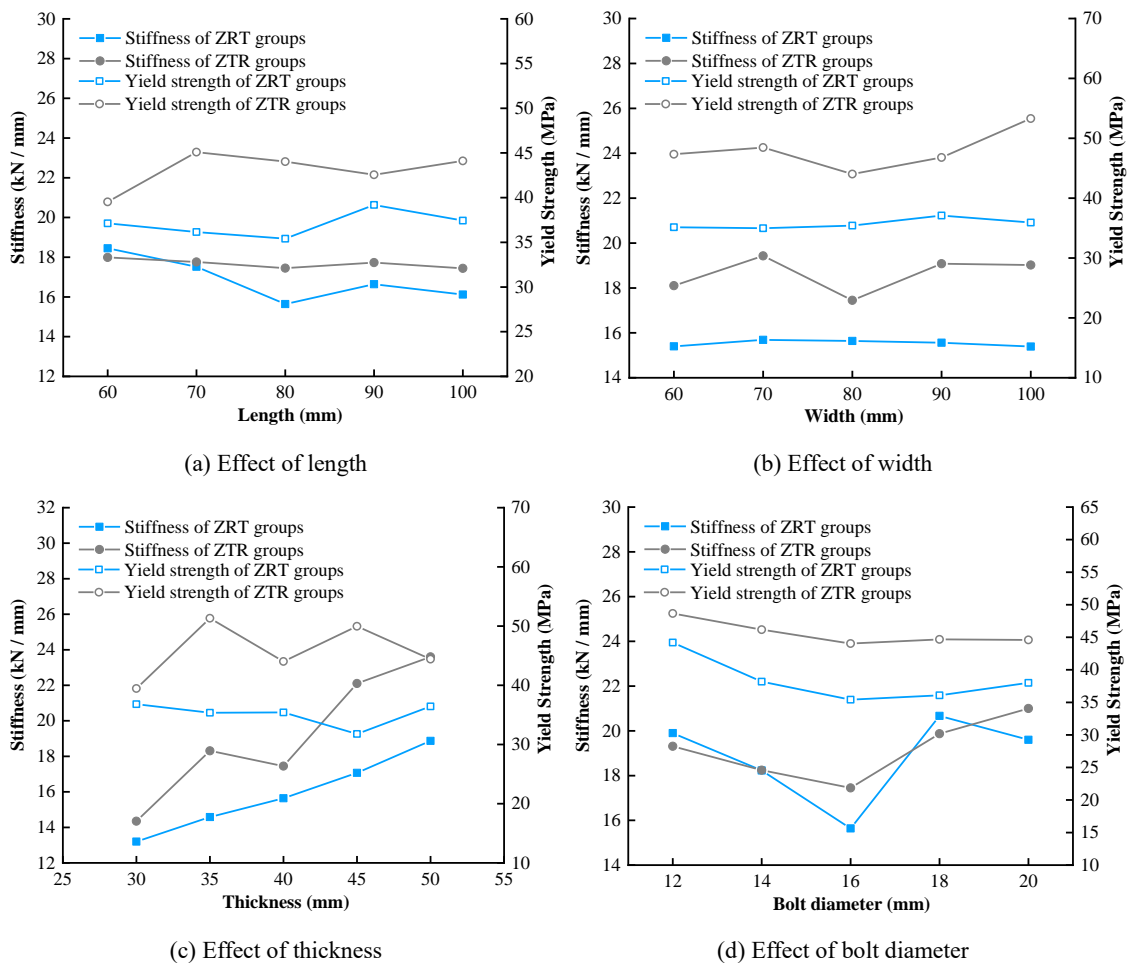(c) Effect of thickness

(d) Effect of bolt diameter

Fig. 15 Diagram of factors effecting perpendicular-to-grain dowel-bearing properties

Fig. 15 (b) reveals that when the width increases, the stiffness, and the strength of the specimens are

unchanged. However, for ZTR groups, the yield strength of the specimens at the width of 80 mm is lower because of the lack of stiffness.

From Fig. 15 (c), it can be seen that the thickness has a significant effect on the stiffness of the specimens, and the stiffness generally increases with the increase of the thickness. Since stiffness refers to the ability of a material to resist deformation under external forces, it is obvious that the thicker the specimen is, the higher the stiffness will be. The thickness has little effect on the yield strength of the specimens. At first, the stress distribution of the bearing section of the dowel along the thickness was uneven, but after the local plastic deformation occurred, the internal stress was redistributed, so the bearing strength remained unchanged with the increase in thickness.

In summary, the stiffness of the specimens increases with the increase in thickness, and the width and length have little effect on it. The size of the specimens has no significant influence on the yield strength. According to the parameters and results of this test, it is recommended that the size of the side pressure LBL perpendicular-to-grain dowel-bearing strength specimen is L ≥ 5D, W ≥ 5D and T ≥ 3D. In this case, the size of specimens has a negligible effect on the bearing strength. The result is consistent with that proposed by Wilkinson [36], who believes that the sample size will not affect the bearing strength if under the premise of meeting the minimum size.

3.4 Bolt diameter effect

Through Fig. 15 (d), it is found that in the range of 12 ~ 16 mm, the stiffness decreases with the increase of bolt diameter from 16 mm to 20 mm. Overall, the stiffness of the specimens decreases first and then increases, and reaches the minimum value of 16 mm. Hwang et al. [27] and Ramirez et al. [5] studied the dowel-bearing specimens made of LBL, and found that the stiffness of the specimen decreased with the increase of bolt diameter, while the test results of Rammer [31] were different, it found that the stiffness of the specimen increased with the bolt diameter at the beginning, and then gradually stabilized. The reason for this difference may be explained by the different structures of the laminated material and the original material. The laminated material is composed of minor specification units through transverse and longitudinal bonding, and there is also the influence of the adhesive layer on the mechanical properties of the specimens.

The yield strength of specimens decreases with the increase of the bolt diameter and is stable after the bolt diameter of 16 mm. With the increase in bolt diameter, the relative effective force volume of the specimen decreased, resulting in a decrease in yield strength. However, when the diameter continued to

increase, the force range of the specimen under the bolt also continued to increase, and the force concentration phenomenon was avoided. Therefore, the impact of these two aspects on the yield strength of the specimen was offset, and the yield strength tended to be stable. Rammer [31] pointed out that the dowel-bearing strength decreased with the increase of the bolt diameter, but there was no significant difference in the dowel-bearing strength for the specimen with a large bolt diameter, which was consistent with our test. Sawata and Yasumura [32] also observed this phenomenon in the test of perpendicular-to-grain wood specimens. This phenomenon indicates that the bolt joints designed with small diameters have greater safety reserve than that with large diameters.

3.5 Bamboo unit arrangement effect

It can be seen from Fig. 16 (d) that the stiffness of most specimens with ZTR arrangement is higher than that with ZRT arrangement regardless of the influence of those four factors. This is because the elastic modulus of ZTR specimens with the same bamboo arrangement is higher than that of ZTR specimens, so ZTR specimen with the same bamboo arrangement shows higher stiffness in the dowel-bearing test. The yield strength of all specimens with the ZTR arrangement is higher than that with the ZRT arrangement.

Related to the failure modes of the specimens with those two kinds of arrangements, ZTR specimens have higher stiffness and strength, and the ductility performance is also better than that of ZTR specimens. This phenomenon can be a consequence of their differences in failure modes. The failure of ZTR specimens is mainly due to the cracking of the adhesive layer, while the cracks of ZRT specimens are located in interior bamboo fiber. The adhesive layer is the weak part of the side pressure LBL, which can explain why the mechanical performance of the ZTR specimen is weaker than that of the ZRT specimen. Therefore, it is recommended to use the ZTR arrangement in engineering, which can improve the mechanical properties of bolted joints and be more economical and environmentally friendly.

4 Calculation

4.1 Prediction and applicability of the current formula

The current calculation formula of wood dowel-bearing strength is mainly based on the reference to ANSI / NDS [37] or EN 1995-1-1 [38]. According to ANSI / NDS [37], the theoretical calculation formula for the dowel-bearing strength of wood is provided related to the specific gravity of wood and the diameter of bolts (Eq. (2)). EN 1995-1-1 [38] has a comprehensive design for dowel-bearing strength, which is based on the bolt diameter and material density. For different types of wood-based composites, there are three corresponding formulas for different wooden materials of diverse densities: softwood, laminated veneer

lumber (LVL), and hardwood (Eq. (3)).

$$f_c = 212G^{1.45}D^{-0.5} \tag{2}$$

Where f_c is perpendicular-to-grain dowel-bearing strength (MPa), G is the specific gravity of the material, and D is the bolt diameter (mm).

$$f_c = \frac{0.082(1-0.01d)\rho_k}{k_{90}} \tag{3}$$

$$k_{90} = \begin{cases} 1.35 + 0.015d & \text{(Softwood)} \\ 1.30 + 0.015d & \text{(LVL)} \\ 0.90 + 0.015d & \text{(Hardwood)} \end{cases}$$

Where f_c is perpendicular-to-grain dowel-bearing strength (MPa), d is the bolt diameter (mm), *and* ρ_k is material density (kg / m³).
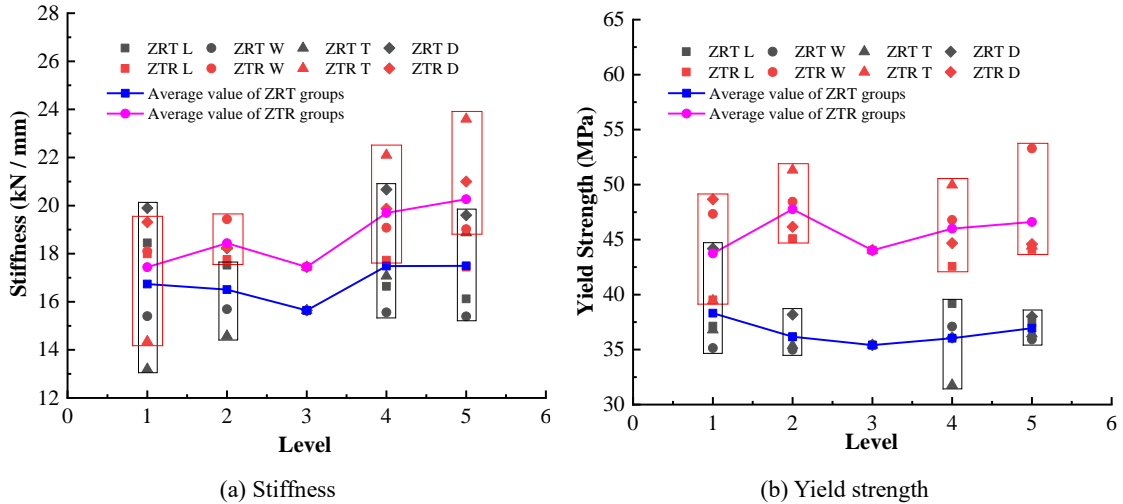
Note：1. The length range of the rectangular represents the coverage of the specimen's test value. 2. Horizontal coordinates represent the five levels of four different effect factors.

Fig. 16 Comparison of bamboo unit arrangement for perpendicular-to-grain dowel-bearing properties

Considering that the properties of the ZTR arrangement are better than that of the ZRT arrangement, the ZRT arrangement should be avoided in practical application, so the applicability of the formula prioritizes ZTR arrangement specimens. Depending on Fig. 17, the value of perpendicular-to-grain dowel-bearing strength forecasted by ANSI / NDS and EN 1995-1-1 is significantly smaller, except for the hardwood formulas in EN 1995-1-1, whose computations are similar to the results of current experiments. This is because the bi-directionality of bamboo is more obvious than that of wood, and the vascular bundle bearing capacity of bamboo in the perpendicular-to-grain direction is stronger, while the other two formulas are based on wood with low density (0.36 ~ 0.52 g / cm³) without considering the applicability to high-density wood. The density of side pressure LBL was 0.672 g / cm³, which was close to the density of

hardwood. The formula was inspired by the material density and the bolt diameter. Therefore, the formula in EN 1995-1-1 for calculating the perpendicular-to-grain dowel-bearing strength of hardwood was the most consistent with the results of this test data.
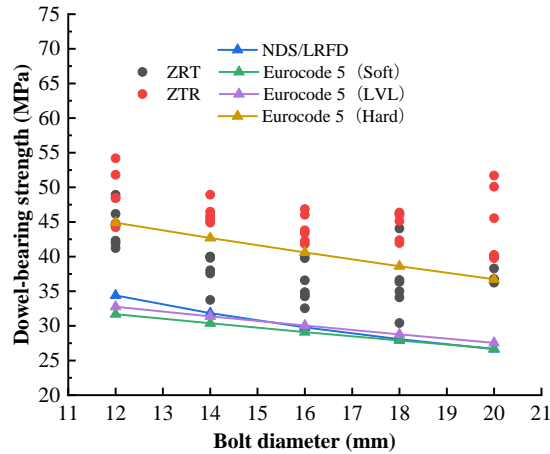

Fig. 17 Comparison between the test results and the predicted values of the current formula

The bearing strength calculated using the formula showed a downward trend with the increase in the bolt diameter. However, only in the range of 12 mm ~ 16 mm of the bolt diameter, it had the same trend as the predicted data. Although the yield strength of ZRT specimens obtained by the 5 % D offset method is greater than the predicted value of the formula, from the perspective of safety reserve, the formula was applicable in the 12 mm ~ 20 mm range of bolt diameter.

4.2 Optimization and construction of the theoretical formula

Through the comparison between the current formula and the test result, the formula applied to hardwood in EN 1995-1-1 applies to predict the perpendicular-to-grain dowel-bearing strength of side pressure LBL, but for the specimens of larger bolt diameter, the degree of anastomosis is poor. Therefore, based on the current formula, the optimization analysis was performed, and the theoretical formula for calculating perpendicular-to-grain dowel-bearing strength of side pressure LBL was constructed.

The density of LBL is uniform and there is no difference in density grade, the density parameter can not be directly introduced into the new formula, but the current formula is based on density and bolt diameter. To solve this problem, drawing on Long's [39] design concepts, the compressive strength of the material is introduced. Because of the great correlation between the bearing strength and density of the material, this is equivalent to taking into account the influence of density. Nevertheless in this book, the formula of dowel-bearing strength is based on the compressive strength of the wood multiplied by the corresponding reduction coefficient, without considering the influence of bolt diameter.

According to the perpendicular-to-grain compressive test, the compressive strength of ZRT and ZTR

arranged in the same batch of side pressure LBL was measured to be 20.52 MPa and 24.96 MPa, respectively. To verify the relationship between the compressive strength and the dowel-bearing strength in the perpendicular-to-grain direction of side pressure LBL, those two kinds of strength are compared in Table 3. The ratio of compressive strength of ZRT and ZTR specimen (0.8221) was used as the test mean, and the ratio of dowel-bearing strength was tested by the one-sample-t-test method. The test results show that the probability $P > |t| = 0.40566 > 0.05$ at the 0.05 level, which indicates that there is no significant difference between the sample and the mean value, it means that the compressive strength is proportional to the dowel-bearing strength in the perpendicular-to-grain direction of side pressure LBL. It also explains that the behavior of introducing compressive strength into the formula for dowel-bearing strength is completely feasible.

Table 3 Comparison between compressive strength and dowel-bearing strength

Specimen types		Value of Strength (MPa)		Ratio
		ZRT	ZTR	
Compression specimen		20.52	24.96	0.8221
Dowel-bearing strength specimen	D12	44.19	48.66	0.9081
	D14	38.18	46.17	0.8269
	D16	35.41	44.03	0.8042
	D18	36.09	44.68	0.8077
	D20	38.00	44.59	0.8522

A theoretical formula of perpendicular-to-grain dowel-bearing strength of side pressure LBL (Eq. 4) was proposed. When the size of the specimens (length, width, and thickness) meets the minimum requirements, the size effect is not obvious. Therefore, the new formula does not consider the size effect, and the dowel-bearing strength is mainly affected by the diameter of the bolt and the arrangement of bamboo. The different arrangement of bamboo affects the compressive properties of the material physically. Therefore, the bolt diameter and the perpendicular-to-grain compressive strength of the material were taken as the factors to construct the theoretical formula.

$$f_y = f_c(ae^{k_d D} + b) \tag{4}$$

Where f_y is dowel-bearing strength (MPa), f_c is compressive strength (MPa), k_d is the bolt diameter influence index, D is bolt diameter (mm), and a and b are constants.

Depending on the 10 groups of data listed in Table 3, the results of 5 groups of ZTR specimens were selected for regression fitting (Eq. 5), and the results of 5 groups of ZRT specimens were used to verify the fitting results (Fig. 18, Table 4). The purpose of the fitting mode was to better coincide the fitting curve with the results of ZTR specimens since ZTR arrangement was recommended in engineering. The

verification results show that the error between the predicted value and the actual value is small, the minimum error is 1.04 %, and the maximum error is 8.9 %, which indicates that the theoretical formula can accurately predict the perpendicular-to-grain dowel-bearing strength of side pressure LBL.

$$f_{y,90} = f_{c,90}(141e^{-0.55D} + 1.77) \tag{5}$$

Where $f_{y,90}$ is perpendicular-to-grain dowel-bearing strength (MPa), $f_{c,90}$ is perpendicular-to-grain compressive strength (MPa), and D is bolt diameter (mm).

Table 4 Validation and error analysis of fitting results

Fitting groups	Dowel-bearing strength (MPa)			Validation groups	Dowel-bearing strength (MPa)		
	Test value	Theoretical value	Error (%)		Test value	Theoretical value	Error (%)
ZTRD12	48.66	48.97	0.63	ZRTD12	44.19	40.26	8.90
ZTRD14	46.17	45.77	0.86	ZRTD14	38.18	37.63	1.44
ZTRS	44.03	44.71	1.54	ZRTS	35.41	36.76	3.80
ZTRD18	44.68	44.36	0.73	ZRTD18	36.09	36.47	1.04
ZTRD20	44.59	44.24	0.79	ZRTD20	38	36.37	4.29

Note：error = [| (theoretical value − test value) | / test value] × 100 %
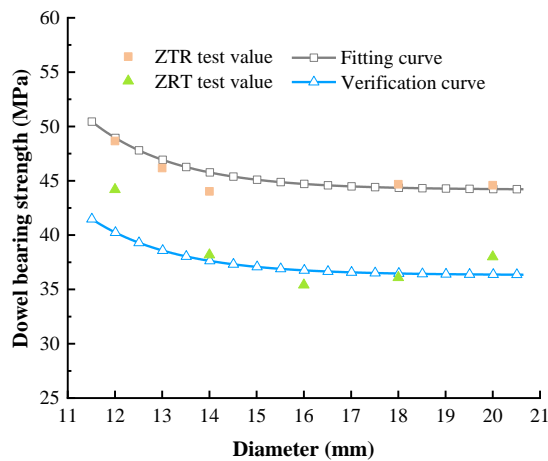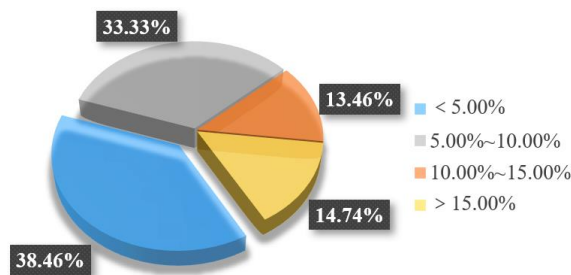

Fig. 18 Fitting curve and verification curve

Fig. 19 Error analysis of the 16 mm specimens

According to the results of the test, the size of the specimen has no significant effect on perpendicular-to-grain dowel-bearing strength. Therefore, the dowel-bearing strength of all the specimens with the same diameter of 16 mm should be consistent with the calculation results of the theoretical formula. The statistical

and error analysis of 156 specimens with a diameter of 16 mm was carried out by using the same method as Table 4, and the results were divided into four error levels: error ＜ 5.00 %, 5.00 ~ 10.00 %，10.00 % ~ 15.00 % and error ＞ 15.00 % (Fig. 19). The specimens with an error less than 5.00 % accounted for 38.46 %, which was the highest in the four grades. The specimens with an error of less than 15.00 % reached 85.26 %, and only 14.74 % of the specimens have an error of more than 15.00 %. The data shows that the theoretical formula is available for predicting the perpendicular-to-grain dowel-bearing strength of side pressure LBL.

5 Conclusions

In this research, the size effect (length, width, and thickness), the bolt diameter, and the arrangement of the bamboo unit were taken into account to study the perpendicular-to-grain dowel-bearing behavior of side pressure LBL. Based on the current formula for calculating the perpendicular-to-grain dowel-bearing strength of wooden materials, a formula suitable for side pressure LBL was constructed, and the following conclusions were obtained:

(1) When the size of the specimens meets the conditions of L ≥ 5D, W ≥ 5D, and T ≥ 3D, it has little effect on the dowel-bearing strength. The width and length of the specimens do not affect the stiffness, and the increase in thickness can increase the ability of the specimen to resist external deformation.

(2) When the bolt diameter changes from 12 mm to 20 mm, the stiffness of the pattern decreases first and then increases, reaching a minimum of 16 mm. The dowel-bearing strength decreases with the increase in bolt diameter and tends to be stable at 16 mm.

(3) The lateral cracks of the 2 bamboo arrangements of ZRT and ZTR can be divided into six different modes. The adhesive layer between the bamboo laminates plays a decisive role when ZRT specimens are destroyed, while it is mainly the tensile or shear failure of the bamboo fiber itself when ZTR specimens are broken.

(4) The bearing performance of ZTR specimens is better than that of ZRT specimens, so the arrangement of ZTR is recommended applying to the bolted joints components of side pressure LBL, which can achieve better mechanical properties, more economical and practical, and ensure the safety of bamboo structure to a certain extent.

(5) The formula in ANSI / NDS and EN 1995-1-1 was used to predict the perpendicular-to-grain dowel-bearing strength in current research, but the results were generally small, except that the predicted values used for hardwood in EN 1995-1-1 are somehow consistent with the test. On this basis, the

theoretical formula suitable for perpendicular-to-grain dowel-bearing strength of side pressure LBL was reconstructed: $f_{y,90} = f_{c,90} (141e^{-0.55D} + 1.77)$. The number of specimens whose error with the test value is less than 15 % accounts for 85.26 % of the total.

Authorship contribution statement

Tingting Ling: Test, Investigation, Formal analysis, Writing-original draft. Haitao Li: Conceptualization, Funding acquisition, Formal analysis, Investigation, Formal analysis, Writing-original draft. Gensheng Cheng: Test, Investigation. Zhenhua Xiong: Funding acquisition, Supervision. Rodolfo Lorenzo: Investigation, Writing-review & editing.

Declaration of competing interest

The authors declare that they have no known competing financial interests or personal relationships that could have appeared to influence the work reported in this paper.

Acknowledgments

References

[1] KW Liu, D Jayaraman, YJ Shi, K Harries, J Yang, et al. "Bamboo: a very sustainable construction material"-2021 International Online Seminar summary report. Sustainable Structures, 2022, 2(1): 000015. https://doi.org/10.54113/j.sust.2022.000015.

[2] DY Zhang, M Gong, SJ Zhang, XD Zhu. A review of tiny houses in North America: Market demand. Sustainable Structures, 2022, 2(1): 000012. https://doi.org/10.54113/j.sust.2022.000012.

[3] P van der Lugt, AAJF van den Dobbelsteen, JJA Janssen. An environmental, economic, and practical assessment of bamboo as a building material for supporting structures. Construction and Building Materials, 2006, 20(9): 648-656. https://doi.org/10.1016/j.conbuildmat.2005.02.023.

[4] D Awalluddin, MAM Ariffin, MH Osman, MW Hussin, MA Ismail, et al. Mechanical properties of different bamboo species. Matec Web of Conferences, 2017, 138: 1024. https://doi.org/10.1051/matecconf/201713801024.

[5] F Ramirez, JF Correal, LE Yamin, JC Atoche, CM Piscal. Dowel-bearing strength behavior of glued laminated guadua bamboo. Journal of Materials in Civil Engineering, 2012, 24 (11): 1378-1387.

[6] XF Sun, MJ He, Z Li. Novel engineered wood and bamboo composites for structural applications: state-of-art of manufacturing technology and mechanical performance evaluation. Construction and Building Materials, 2020, 249. https://doi.org/10.1016/j.conbuildmat.2020.118751.

[7] M Mahdavi, PL Clouston, SR Arwade. Development of laminated bamboo lumber: review of processing, performance, and economical considerations. Journal of Materials in Civil Engineering, 2011, 23(7): 1036-1042. https://doi.org/10.1061/(ASCE)MT.1943-5533.0000253.

[8] Y Xiao, RZ Yang, B Shan. Production, environmental impact and mechanical properties of glubam. Construction and Building Materials, 2013, 44(7): 765-773. https://doi.org/10.1016/j.conbuildmat.2013.03.087.

[9] J Liu, AP Zhou, BL Sheng, YY Liu, LW Sun. Effect of temperature on short-term compression creep property of bamboo scrimber. Journal of Forestry Engineering, 2021, 6(2): 64-69. https://doi.org/10.13360/j.issn.2096-1359.202006003.

[10] YJ Li, ZC Lou. Progress of bamboo flatten technology research. Journal of Forestry Engineering, 2021, 6(4): 14-23. https://doi.org/10.13360/j.issn.2096-1359.202012021.

[11] HR Liu, XM Yang, XB Zhang, Q Su, FD Zhang et al. The tensile shear bonding property of flattened bamboo sheet. Journal of Forestry Engineering, 2021, 6(1): 68-72. https://doi.org/10.13360/j.issn.2096-1359.202005029.

[12] F Xiao, YQ Wu, YF Zuo, L Peng, WH Li, et al. Preparation and bonding performance evaluation of bamboo veneer/foam aluminum composites. Journal of Forestry Engineering, 2021, 6(3): 35-40. https://doi.org/10.13360/j.issn.2096-1359.202009024.

[13] WC Lei, YM Zhang, WJ Yu, YL She. The adsorption and desorption characteristics of moso bamboo induced by heat treatment. Journal of Forestry Engineering, 2021, 6(3): 41-46. https://doi.org/10.13360/j.issn.2096-1359.202010008.

[14] M Lobovikov. Bamboo and rattan products and trade. Journal of Bamboo and Rattan, 2003 2(4): 397-406. https://doi.org/10.1163/156915903322700421.

[15] GS Yang. Bamboo-from raw bamboo to glued laminated bamboo structure. Hans Journal of Civil Engineering, 2020, 09(7): 623-635. https://doi.org/10.12677/HJCE.2020.97067.

[16] A Dauletbek, HT Li, ZH Xiong, R Lorenzo. A review of mechanical behavior of structural laminated bamboo lumber. Sustainable Structures, 2021, 1(1): 000004. https://doi.org/10.54113/j.sust.2021.000004.

[17] HT Li, QS Zhang, DS Huang, AJ Deeks. Compressive performance of laminated bamboo. Composites Part B: Engineering, 2013, 54(1): 319-328. https://doi.org/10.1016/j.compositesb.2013.05.035.

[18] HT Li, W Xu, C Chen, LS Yao, R Lorenzo. Temperatures influencing on the bending performance of laminated bamboo lumber. Journal of Materials in Civil Engineering ASCE, 2022, accepted. https://doi.org/1

0.1061/(ASCE)MT.1943-5533.0004730.

[19] IM Sulastiningsih. Physical and mechanical properties of laminated bamboo board. Journal of Tropical Forest Science, 2009, 21(3): 246-251. https://doi.org/10.2307/23616804.

[20] CS Verma, NK Sharma, VM Chariar, S Maheshwari, MK Hada. Comparative study of mechanical properties of bamboo laminae and their laminates with woods and wood based composites. Composites Part B: Engineering, 2014, 60: 523-530. https://doi.org/10.1016/j.compositesb.2013.12.061.

[21] HT Li, B Chen, BH Fei, H Li, ZH Xiong, et al. Mechanical properties of aramid fiber reinforced polymer confined laminated bamboo lumber column under cyclic loading. European Journal of Wood and Wood Products, 2022, 80: 1057-1070. https://doi.org/10.1007/s00107-022-01816-4.

[22] MAM Quintero, CPT Tam, HT Li. Structural analysis of a Guadua bamboo bridge in Colombia. Sustainable Structures, 2022, 2(2): 000020. https://doi.org/10.54113/j.sust.2022.000020.

[23] JW Su, HT Li, ZH Xiong, R Lorenzo. Structural design and construction of an office building with laminated bamboo lumber. Sustainable Structures, 2021, 1(2): 000010. https://doi.org/10.54113/j.sust.2021.000010.

[24] P Dietsch, R Brandner. Self-tapping screws and threaded rods as reinforcement for structural timber ele ments-a state-of-the-art report. Construction and Building Materials, 2015, 97: 78-89. https://doi.org/10.1016/j.conbuildmat.2015.04.028.

[25] I Smith, LRJ Whale, C Anderson, BO Hilson, PD Rodd. Design properties of laterally loaded nailed or bolted wood joints. Canadian Journal of Civil Engineering, 1988, 15(4): 633-643. https://doi.org/10.1139/l88-085.

[26] DR Rammer, SG Winistorfer. Effect of moisture content on dowel-bearing strength. Wood and Fiber Science, 2001, 33(1): 126-139.

[27] K Hwang, K Komatsu. Bearing properties of engineered wood products I: effects of dowel diameter and loading direction. Journal of Wood Science, 2002, 48(4): 295-301. https://doi.org/10.1007/BF00831350.

[28] MAS Zitto, J Kohler, JC Piter. Embedding strength in joints of fast-growing Argentinean eucalyptus grandis with dowel-type fasteners. Analysis according to the criterion adopted by European Standards. European Journal of Wood and Wood Products, 2012, 70(4): 433-440. https://doi.org/10.1007/s00107-011-0572-9.

[29] HT Li, TY Gao, GS Cheng, R Lorenzo. Evaluation on the pin groove compressive performance of laminated bamboo lumber at different angles. Cellulose, 2022, accepted. https://doi.org/10.1007/s10570-022-04920-z.

[30] JHP Quenneville, M Mohammad. On the failure modes and strength of steel-wood-steel bolted timber connections loaded parallel-to-grain. Canadian Journal of Civil Engineering, 2000, 27(4): 761-773. https://doi.org/10.1139/cjce-27-4-761.

[31] DR Rammer. Parallel-to-grain dowel-bearing strength of two Guatemalan hardwoods. Forest Products Journal, 1999, 49(6): 77-87. https://doi.org/10.1023/A:1009223516957.

[32] K Sawata, M Yasumura. Determination of embedding strength of wood for dowel-type fasteners. Journal of Wood Science, 2002, 48(2): 138-146. https://doi.org/10.1007/BF00767291.

[33] F Lam, M Gehloff, M Closen. Moment-resisting bolted timber connections. Proceedings of the Institution of Civil Engineers: Structures and Buildings, 2010, 163(4): 267-274. https://doi.org/10.1680/stbu.2010.163.4.267.

[34] American Society for Testing and Materials. Standard test method for evaluating dowel-bearing strength of wood and wood-based products. ASTM D5764, 2007.

[35] Timber Structures-Test methods-Determination of embedment strength and foundation values for dowel type fasteners. BS EN 383-2007, 2007.

[36] TL Wilkinson. Dowel-bearing Strength. Forest Products Laboratory, Madison, Wisconsin, 1991.

[37] American wood council. National design specification for wood construction. ANSI/NDS SUPP-2018, 2018.

[38] E Standardization. Eurocode 5: design of timber structures. part 1-1: general common rules and rules for buildings. EN 1995-1-1, 124, 2004.

[39] W. Long. Design of timber structure, fourth ed. China Architecture and Building Press, 2005. (in Chinese)